

Near-threshold Photoproduction of ϕ Mesons from Deuterium

X. Qian,^{1,2} W. Chen,¹ H. Gao,¹ K. Hicks,³ K. Kramer,¹ J.M. Laget,⁴ T. Mibe,³ Y. Qiang,¹ S. Stepanyan,⁴
 D.J. Tedeschi,⁵ W. Xu,⁶ K.P. Adhikari,³³ M. Amaryan,³³ M. Anghinolfi,²⁴ J. Ball,¹⁴ M. Battaglieri,²⁴
 V. Batourine,⁴ I. Bedlinskiy,²⁷ M. Bellis,¹² A.S. Biselli,^{18,12} C. Bookwalter,²⁰ D. Branford,¹⁷ W.J. Briscoe,²¹
 W.K. Brooks,^{39,4} V.D. Burkert,⁴ S.L. Careccia,³³ D.S. Carman,⁴ P.L. Cole,^{22,4} P. Collins,^{8,*} V. Crede,²⁰
 A. D'Angelo,^{25,36} A. Daniel,³ N. Dashyan,⁴² R. De Vita,²⁴ E. De Sanctis,²³ A. Deur,⁴ B. Dey,¹² S. Dhamija,¹⁹
 C. Djalali,⁵ D. Doughty,^{15,4} R. Dupre,⁷ H. Egiyan,³¹ A. El Alaoui,⁷ P. Eugenio,²⁰ S. Fegan,⁴⁰ M.Y. Gabrielyan,¹⁹
 N. Gevorgyan,⁴² G.P. Gilfoyle,³⁵ K.L. Giovanetti,²⁸ F.X. Girod,^{14,†} J.T. Goetz,⁹ W. Gohn,¹⁶ R.W. Gothe,⁵
 L. Graham,⁵ K.A. Griffioen,⁴¹ M. Guidal,²⁶ L. Guo,^{4,‡} K. Hafidi,⁷ H. Hakobyan,^{39,42} C. Hanretty,²⁰ N. Hassall,⁴⁰
 M. Holtrop,³¹ Y. Ilieva,^{5,21} D.G. Ireland,⁴⁰ S.S. Jawalkar,⁴¹ H.S. Jo,²⁶ K. Joo,^{16,39} D. Keller,³ M. Khandaker,³² P.
 Khetarpal,¹⁹ A. Kim,²⁹ W. Kim,²⁹ A. Klein,³³ F.J. Klein,¹³ P. Konczykowski,¹⁴ V. Kubarovsky,^{4,34}
 S.V. Kuleshov,^{39,27} V. Kuznetsov,²⁹ K. Livingston,⁴⁰ D. Martinez,²² M. Mayer,³³ J. McAndrew,¹⁷
 M.E. McCracken,¹² B. McKinnon,⁴⁰ C.A. Meyer,¹² K. Mikhailov,²⁷ T. Mineeva,¹⁶ M. Mirazita,²³ V. Mokeev,^{37,4}
 B. Moreno,¹⁴ K. Moriya,¹² B. Morrison,⁸ H. Moutarde,¹⁴ E. Munevar,²¹ P. Nadel-Turonski,⁴ A. Ni,²⁹ S. Niccolai,²⁶
 I. Niculescu,²⁸ M.R. Niroula,³³ M. Osipenko,²⁴ A.I. Ostrovidov,²⁰ R. Paremuzyan,⁴² K. Park,^{5,29,†} S. Park,²⁰ S.
 Anefalos Pereira,²³ S. Pisano,²⁶ O. Pogorelko,²⁷ S. Pozdniakov,²⁷ J.W. Price,¹⁰ S. Procureur,¹⁴ D. Protopopescu,⁴⁰
 G. Ricco,²⁴ M. Ripani,²⁴ B.G. Ritchie,⁸ G. Rosner,⁴⁰ P. Rossi,²³ F. Sabatié,¹⁴ M.S. Saini,²⁰ C. Salgado,³²
 D. Schott,¹⁹ R.A. Schumacher,¹² E. Seder,¹⁶ H. Seraydaryan,³³ Y.G. Sharabian,⁴ E.S. Smith,⁴ G.D. Smith,⁴⁰
 D.I. Sober,¹³ D. Sokhan,²⁶ S.S. Stepanyan,²⁹ P. Stoler,³⁴ I.I. Strakovsky,^{21,§} S. Strauch,^{5,21} M. Taiuti,²⁴
 C.E. Taylor,²² S. Tkachenko,⁵ M. Ungaro,^{16,34} B. Vernarsky,¹² M.F. Vineyard,³⁸ E. Voutier,³⁰ L.B. Weinstein,³³
 D.P. Weygand,⁴ M.H. Wood,^{11,5} N. Zachariou,²¹ L. Zana,³¹ J. Zhang,³³ B. Zhao,^{16,¶} and Z.W. Zhao⁵

(The CLAS Collaboration)

¹Duke University, Durham, North Carolina 27708

²Kellogg Radiation Laboratory, California Institute of Technology, California 91125

³Ohio University, Athens, Ohio 45701

⁴Thomas Jefferson National Accelerator Facility, Newport News, Virginia 23606

⁵University of South Carolina, Columbia, South Carolina 29208

⁶Massachusetts Institute of Technology, Cambridge, Massachusetts 02139-4307

⁷Argonne National Laboratory, Argonne, Illinois 60441

⁸Arizona State University, Tempe, Arizona 85287-1504

⁹University of California at Los Angeles, Los Angeles, California 90095-1547

¹⁰California State University, Dominguez Hills, Carson, CA 90747

¹¹Canisius College, Buffalo, NY

¹²Carnegie Mellon University, Pittsburgh, Pennsylvania 15213

¹³Catholic University of America, Washington, D.C. 20064

¹⁴CEA, Centre de Saclay, Irfu/Service de Physique Nucléaire, 91191 Gif-sur-Yvette, France

¹⁵Christopher Newport University, Newport News, Virginia 23606

¹⁶University of Connecticut, Storrs, Connecticut 06269

¹⁷Edinburgh University, Edinburgh EH9 3JZ, United Kingdom

¹⁸Fairfield University, Fairfield CT 06824

¹⁹Florida International University, Miami, Florida 33199

²⁰Florida State University, Tallahassee, Florida 32306

²¹The George Washington University, Washington, DC 20052

²²Idaho State University, Pocatello, Idaho 83209

²³INFN, Laboratori Nazionali di Frascati, 00044 Frascati, Italy

²⁴INFN, Sezione di Genova, 16146 Genova, Italy

²⁵INFN, Sezione di Roma Tor Vergata, 00133 Rome, Italy

²⁶Institut de Physique Nucléaire ORSAY, Orsay, France

²⁷Institute of Theoretical and Experimental Physics, Moscow, 117259, Russia

²⁸James Madison University, Harrisonburg, Virginia 22807

²⁹Kyungpook National University, Daegu 702-701, Republic of Korea

³⁰LPSC, Université Joseph Fourier, CNRS/IN2P3, INPG, Grenoble, France

³¹University of New Hampshire, Durham, New Hampshire 03824-3568

³²Norfolk State University, Norfolk, Virginia 23504

³³Old Dominion University, Norfolk, Virginia 23529

³⁴Rensselaer Polytechnic Institute, Troy, New York 12180-3590

³⁵University of Richmond, Richmond, Virginia 23173

³⁶*Universita' di Roma Tor Vergata, 00133 Rome Italy*

³⁷*Skobeltsyn Nuclear Physics Institute, Skobeltsyn Nuclear Physics Institute, 119899 Moscow, Russia*

³⁸*Union College, Schenectady, NY 12308*

³⁹*Universidad Técnica Federico Santa María, Casilla 110-V Valparaíso, Chile*

⁴⁰*University of Glasgow, Glasgow G12 8QQ, United Kingdom*

⁴¹*College of William and Mary, Williamsburg, Virginia 23187-8795*

⁴²*Yerevan Physics Institute, 375036 Yerevan, Armenia*

(Dated: March 13, 2019)

We report the first measurement of the differential cross section on ϕ -meson photoproduction from deuterium near the production threshold for a proton using the CLAS detector and a tagged-photon beam in Hall B at Jefferson Lab. The measurement was carried out by a triple coincidence detection of a proton, K^+ and K^- near the theoretical production threshold of 1.57 GeV. The extracted differential cross sections $\frac{d\sigma}{dt}$ for the initial photon energy from 1.65-1.75 GeV are consistent with predictions based on a quasifree mechanism. This experiment establishes a baseline for a future experimental search for an exotic ϕ -N bound state from heavier nuclear targets utilizing subthreshold/near-threshold production of ϕ mesons.

PACS numbers: 13.60.Le, 24.85.+p, 25.10.+s, 25.20.-x

It is expected that quark-exchange interactions are strongly suppressed when there are no common valence quarks between two interacting hadrons. Therefore, interactions between vector mesons (e.g. ϕ and J/ψ mesons) and nucleons are a rich source of information on the role of glue in the confinement region. These processes have been studied for decades [1]. The presence of the attractive QCD van der Waals interaction, proposed by Brodsky, Schmidt and de Téramond [2], is another manifestation of the role of gluons in the confinement region. The QCD van der Waals interaction, mediated by multi-gluon exchanges, is dominant when two interacting color singlet hadrons have no common valence quarks. Bound states of η_c with ^3He and heavier nuclei were predicted [2, 3]. Similarly, one expects that the attractive QCD van der Waals force also dominates the ϕ -N interaction. A bound state of ϕ -N was found to be possible by Gao, Lee, and Marinov [4]. Such a bound state was also predicted by Huang, Zhang, and Yu using a chiral SU(3) quark model and the extended chiral SU(3) quark model by solving the Resonant Group Method (RGM) equation [5].

To form a ϕ -N bound state, the relative velocity between the ϕ meson and the nucleon needs to be low so that the QCD van der Waals interaction is enhanced [6]. Thus, the experimental search for a ϕ -N bound state can be performed with quasifree subthreshold/near-threshold ϕ -meson photoproduction inside a nucleus, with the subsequent formation of the bound state of the ϕ meson with another nucleon inside the nucleus [4]. The presence of the ϕ -N bound state may lead to a signal in a triple coincidence detection of kinematically correlated K^+ , K^- , and proton in the final state from its decay [4, 7]. The best way to identify it is to adopt a cut on the sum of the momentum magnitudes of K^+ , K^- , and p (about 95% of the incident photon energy E_γ , we take $c=1$), which is confirmed by the simulation studies [8]. The total momentum of the ϕ -N bound state is less than that from

background channels, for example, subthreshold/near-threshold ϕ production without the formation of a bound state and the direct K^+K^- production, and as such, it allows for the separation of the signal from the background.

In this paper, we report on the first measurement of differential cross sections from near-threshold production of ϕ mesons from a deuterium target. The measurement was carried out using the CLAS detector [9] at Jefferson Lab by a triple coincidence detection of K^+ , K^- , and proton. The incident photon energy range used in this analysis is 1.65 - 1.75 GeV, which is above the ϕ -meson photoproduction threshold from a proton target. However, due to the requirement of a triple-coincidence measurement and the imperfect acceptance of the detector, the reconstructed ϕ event in this analysis originated from photoproduction on a high-momentum proton inside the deuteron. These results, therefore, will provide a baseline for a future experimental search for a ϕ -N bound state using heavier nuclear targets, where subthreshold kinematics are important [4].

High statistics data were collected during the CLAS g10 running period [10] from a 24-cm-long liquid-deuterium target. A tagged-photon beam was used, which was generated by a 3.8-GeV electron beam incident on a gold radiator with a thickness of 10^{-4} radiation lengths. The photon flux was measured by the Hall B photon-tagging system [11]. Two settings of the CLAS magnetic field were used during the experiment, corresponding to a low-field setting (with a toroidal magnet current $I=2250$ A) for better forward-angle coverage, and a high-field setting ($I=3375$ A) for better momentum resolution. The reaction $d(\gamma, \phi p)n$ was measured by detecting kaons from the ϕ -meson decay ($\phi \rightarrow K^+K^-$, branching ratio about 0.5), using the same data set as in Refs. [12], [13], and [14].

The K^+ , K^- , and the proton were selected based on the particle charge, momentum, and time-of-flight in-

Run Period	Magnet Current	Target Material	Target Length	Target Position	Accumulated Flux
g10	2250 (A)	LD ₂	24 cm	-25 cm	1.266×10^{12}
g10	2250 (A)	LH ₂	24 cm	-25 cm	7.508×10^{10}
g11	1930 (A)	LH ₂	40 cm	-10 cm	4.316×10^{12}

TABLE I: A comparison of the g10 and g11 experimental settings. The accumulated photon flux is for the E_γ range of 1.65-1.75 GeV. The “-10 cm” means that the target center of the g11 hydrogen target is 10 cm upstream from the nominal center of CLAS.

formation. The reaction $d(\gamma, \phi p)n$ was identified in the missing mass squared distribution by applying a $\pm 3\sigma$ cut on the missing neutron peak. The energy threshold for the $\gamma N \rightarrow \phi N$ reaction is 1.57 GeV. However, due to the minimum detection threshold for charged particles, the CLAS acceptance determined threshold is around 1.75 GeV. This is demonstrated in our analysis as no ϕ events at incident photon energies below 1.75 GeV can be identified from the g10 hydrogen data set, which was taken during the g10 running period for calibration purposes. This finding is consistent with the hydrogen results from the CLAS g11 [15] high statistics data set. Table I summarizes the differences between the g10 and g11 experimental settings. Fig. 1 (left panel) shows the invariant mass distribution of the K^+K^- before the acceptance correction from the g10 deuterium data set, where the ϕ peak is clearly visible. Also shown in Fig. 1 (right panel) is the corresponding spectrum from the g11 hydrogen data set normalized to the g10 integrated luminosity for nucleons. The yield of the g11 hydrogen is ~ 1.5 events per 2.5 MeV around the reconstructed ϕ meson mass, which is strongly suppressed compared to that of the g10 deuteron (~ 23 events per 2.5 MeV) due to the energy threshold of producing a ϕ meson on a nucleon at the kinematic settings of g10 and g11. Therefore, the photon energy range used to extract the near-threshold cross section for ϕ -meson photoproduction from deuterium is between 1.65 GeV and 1.75 GeV in this work. The chosen photon energy range was further confirmed by simulating the $\gamma + p \rightarrow p + \phi$ process for the g10 configuration.

Once the reaction $d(\gamma, pK^+K^-)n$ was identified, the number of ϕ mesons was obtained by subtracting the background under the ϕ peak (invariant mass spectrum of the K^+ and K^-) in the $\pm 3\sigma$ region (see Fig. 1). The K^+K^- invariant mass distribution was fitted using a Breit-Wigner function convoluted with the experimental resolution, plus a function to model the background in each kinematic bin. The experimental resolution on the missing mass ranged from 1.2 to 1.7 MeV for different t bins. They were obtained by fitting the invariant mass distribution of the Monte-Carlo simulation. The

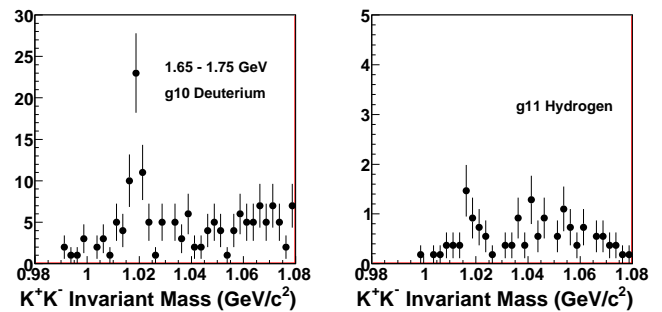


FIG. 1: The K^+K^- invariant mass distribution from the CLAS g10 deuterium data for $E_\gamma = 1.65$ -1.75 GeV (left panel). The x -bin size is 2.5 MeV. The corresponding distribution from the CLAS g11 hydrogen data set in the same photon energy range is shown in the right panel.

background shape was assumed to be [12]:

$$f(x) = a\sqrt{x^2 - (2M_K)^2} + b(x^2 - (2M_K)^2) \text{ for } x > 2M_K$$

$$f(x) = 0 \text{ for } x < 2M_K, \quad (1)$$

where x is the invariant mass of the K^+K^- , M_K is the kaon mass, and a and b are fitting parameters. Such a fit was performed separately for each t bin, and the t dependence of the background was effectively included in the fitting parameters a and b . In addition, the background was also fitted to a straight line. The results from fitting these two shapes were compared in order to estimate the systematic uncertainties due to the subtraction of the background.

GEANT3 Monte-Carlo (MC) simulations were carried out to model detector efficiencies and resolutions for this reaction channel. A quasifree event generator was used for the near-threshold kinematics. It generated pK^+K^- three-body events with a random photon energy based on the photon energy distribution of the data in the energy range of interest. The initial momentum of the nucleon inside the deuteron was chosen using the Bonn potential wavefunction [16]. The spectator nucleon was assumed to be on-shell, whereas the struck nucleon was assumed to be off-shell before absorbing a photon. Isospin symmetry was assumed for the ϕ -meson photoproduction from the nucleon. The events were then checked to ensure energy conservation. The MC events were generated based on a Breit-Wigner shape of the resonance centered at the ϕ mass of 1.019 GeV² with a full width at half maximum (FWHM) of $\Gamma=4.26$ MeV. The ϕ meson decay angular distribution and cross section are based on the g11 hydrogen data [17].

The ϕ -meson differential photoproduction cross section on a hydrogen target ($\frac{d\sigma}{dt}$ vs. $t - t_0$) was obtained using a fit to the g11 data in $E_\gamma = 1.625 - 3.775$ GeV range. Here t is four-momentum transfer squared, $(P_\phi - P_\gamma)^2$, and t_0 is the minimum t value for a given photon energy.

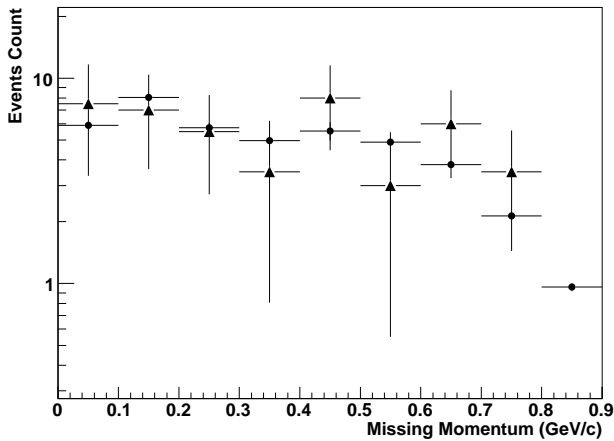


FIG. 2: Missing momentum distributions are shown for data (solid triangles) and MC (solid circles), where the MC results are normalized to the luminosity of the data. Both $\phi - N$ and $N - N$ FSI are included in the Monte Carlo.

In addition, the event generator included the $N - N$ and $\phi - N$ final-state interactions (FSIs). The Jost function approach [18] was used for the $N - N$ FSI. The $\phi - N$ FSI, which was assumed to be incoherent from the original ϕ -meson photoproduction process, was modeled based on the vector meson dominance (VMD) model, in which the t -dependence of the $\phi - N$ elastic scattering cross section is the same as that of ϕ -meson photoproduction. A fitting procedure, in which the strength of $N - N$ and $\phi - N$ FSIs were obtained, was then used to optimize the ϕ -meson photoproduction model so that the resulting Monte-Carlo distributions match those of the data. Fig. 2 shows the comparison in the missing momentum distribution for the data (solid triangles) and the MC (solid circles).

MC-generated events were used as input to the GEANT3-based CLAS simulation [19]. They were then reconstructed using the same algorithm as was used for the data. The acceptance was obtained by the ratio of the number of events that passed the analysis cuts to the number of generated ϕ events. The average differential cross sections were extracted by dividing the normalized yield by the acceptance. The differential cross sections were then bin-centered at fixed t values with a finite binning correction.

Several sources contribute to the overall systematic uncertainty in the differential cross section. The systematic uncertainties associated with particle identification and the missing mass cut were 4.2 - 12.9% and 1.4 - 10.9%, respectively. These values were determined by varying the corresponding cuts by $\pm 10\%$ in each t bin. The angular distributions of the ϕ -meson's decay products in its rest frame and the $\cos(\theta_{c.m.})$ distribution of the ϕ

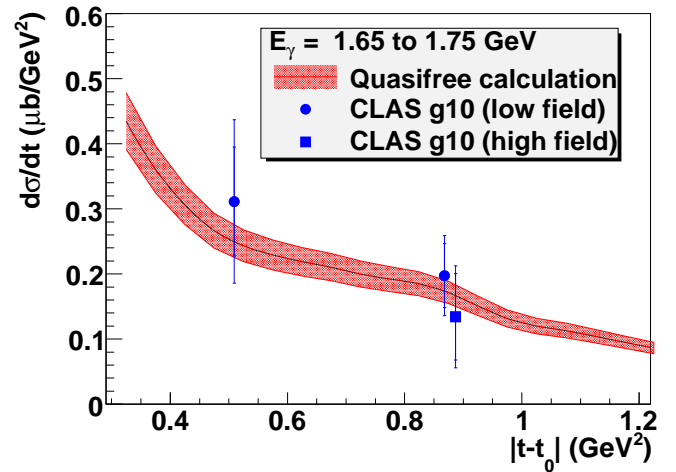


FIG. 3: (Color online) ϕ photoproduction differential cross sections from deuterium are plotted as a function of $|t - t_0|$. The inner error bars are the statistical uncertainties, and the outer error bars are the quadrature sum of systematic and statistical uncertainties.

E_γ (GeV)	$ t - t_0 $ (GeV ²)	$\frac{d\sigma}{dt}$ ($\mu\text{b}/\text{GeV}^2$)	stat. uncer.	sys. uncer.
1.65-1.75	0.509	0.31	0.084	0.094
1.65-1.75	0.887	0.20	0.049	0.037
1.65-1.75	0.924	0.13	0.066	0.041

TABLE II: Tabulated results on the ϕ -meson photoproduction from deuterium for an E_γ range of 1.65 to 1.75 GeV.

meson were uncertain to within 10% and 5% [17, 20], respectively, leading to 5.2-13.2% systematic uncertainties. The background obtained from the non-linear background shape was on average 8% smaller than that from the linear background. A conservative 8% systematic uncertainty is assigned for the background subtraction procedure. The systematic uncertainties due to the effect of FSIs were obtained by varying the fitted strengths of the $N - N$ FSI and the $\phi - N$ FSI by 30% and 50%, respectively. The systematic errors vary from 4% to 17% for different t bins. The uncertainty in the photon flux was 5% [13, 21]. The uncertainty of the bin-centering correction was assumed to be 30% of the size of the correction based on knowledge of the CLAS acceptance and the input cross section model, which is obtained from the g11 data [17]. The absolute size of bin-centering corrections was between 1% and 10%. Combined in quadrature, the overall systematic errors vary from 18% - 32% depending on the kinematics.

The ϕ -meson photoproduction cross sections for the deuteron are tabulated in Table II and are plotted as a function of $|t - t_0|$ in Fig. 3 for a photon energy range of

1.65-1.75 GeV. The solid circles are results obtained from the CLAS g10 low-field setting, whereas the solid square is the result from the high-field setting. The quasifree calculation is also plotted for comparison together with its uncertainty (shown as a band in Fig. 3). This simple calculation is based on a quasifree picture with the ϕ -meson differential photoproduction cross section from the proton which is based on the g11 data [17]. The principle of this calculation is the same as for event generator used in the MC. The systematic uncertainty for this calculation is about 10% due to the uncertainty in the input cross section. The extracted differential cross section for ϕ -meson photoproduction is consistent with the quasifree calculation within uncertainties.

In summary, we have extracted for the first time the differential cross section on ϕ -meson photoproduction from deuterium below the production threshold for the proton accessible on CLAS. The chosen incident photon energy range is 1.65-1.75 GeV, which is near the 1.57 GeV production threshold for protons. Our extracted differential cross sections are in agreement with predictions from a simple quasifree picture. Although heavier nuclear targets will be ideal for future dedicated searches for a ϕ -N bound state, the extracted cross sections from deuterium reported in this paper will help provide reliable information on the expected production rate of the ϕ -N bound state. These data also provide important information on physics backgrounds, such as direct K^+K^- production rates from nucleons.

We acknowledge the outstanding efforts of the staff of the Accelerator and Physics Divisions at Jefferson Lab who made this experiment possible. This work was supported in part by the U.S. Department of Energy, the National Science Foundation, the Italian Istituto Nazionale di Fisica Nucleare, the French Centre National de la Recherche Scientifique and Commissariat à l'Énergie Atomique, and the National Research Foundation of Korea. Jefferson Science Associates (JSA) operates the Thomas Jefferson National Accelerator Facility for the U.S. Department of Energy under contract DE-AC05-06OR23177.

* Current address: Catholic University of America, Washington, D.C. 20064

- [†] Current address: Thomas Jefferson National Accelerator Facility, Newport News, Virginia 23606
- [‡] Current address: Los Alamos National Laboratory, New Mexico, NM
- [§] Current address: The George Washington University, Washington, DC 20052
- [¶] Current address: College of William and Mary, Williamsburg, Virginia 23187-8795
- [1] T. H. Bauer, R. D. Spital, D. R. Yennie, and F. M. Pipkin, *Rev. Mod. Phys.* **50**, 261 (1978); *ibid* **51**, 407(E) (1979); D. G. Cassel *et al.*, *Phys. Rev.* **D24**, 2787 (1981).
- [2] S. J. Brodsky, I. A. Schmidt and G. F. de Téramond, *Phys. Rev. Lett.* **64**, 1011 (1990).
- [3] D. A. Wasson, *Phys. Rev. Lett.* **67**, 2237 (1991).
- [4] H. Gao, T.-S. H. Lee, and V. Marinov, *Phys. Rev. C* **63**, 022201R (2001).
- [5] F. Huang, Z. Y. Zhang, and Y. W. Yu, *Phys. Rev. C* **73**, 025207 (2006).
- [6] M. Luke, A. V. Manohar, and M. J. Savage, *Phys. Lett. B* **288**, 355 (1992).
- [7] S. Liska, H. Gao, W. Chen, and X. Qian, *Phys. Rev. C* **75**, 058201 (2007).
- [8] “First Search for $\phi - N$ Bound State”, Letter of Intent to Jefferson Lab PAC33, LOI-08-004, Spokesperson: Y. Qiang and H. Gao.
- [9] B. A. Mecking *et al.*, *Nucl. Instr. & Meth.* **503/3**, 513 (2003).
- [10] B. McKinnon *et al.* (CLAS Collaboration), *Phys. Rev. Lett.* **96**, 212001 (2006); S. Niccolai *et al.* (CLAS Collaboration), *Phys. Rev. Lett.* **97**, 032001 (2006).
- [11] D. I. Sober *et al.*, *Nucl. Instrum. Methods A* **440**, 263 (2000).
- [12] T. Mibe *et al.* (CLAS Collaboration), *Phys. Rev. C* **76**, 052202R (2007).
- [13] W. Chen *et al.* (CLAS Collaboration), *Phys. Rev. Lett.* **103**, 012301 (2009).
- [14] X. Qian *et al.* (CLAS Collaboration), *Phys. Lett. B* **680**, 417 (2009).
- [15] R. De Vita *et al.* (CLAS Collaboration), *Phys. Rev. D* **74**, 032001 (2006); M. Battaglieri *et al.* (CLAS Collaboration), *Phys. Rev. Lett.* **96**, 042001 (2006).
- [16] R. Machleidt, K. Holinde, and C. Elster, *Phys. Rep.* **149**, 1 (1987).
- [17] D. Tedeschi, *private communication*.
- [18] J. Gillette, *Final-State Interactions* (Holden-Day, San Francisco, 1964).
- [19] http://www.physics.unh.edu/maurik/gsim_info.shtml.
- [20] K. McCormick *et al.* (CLAS Collaboration), *Phys. Rev. C* **69**, 032203 (2004).
- [21] J. Ball and E. Pasyuk, CLAS-NOTE **2005-002** (2005), <http://www1.jlab.org/ul/Physics/Hall-B/clas/public/2005-002.pdf>.